Biochimica et Biophysica Acta 1864 (2016) 738–746

Contents lists available at ScienceDirect

Biochimica et Biophysica Acta

journal homepage: www.elsevier.com/locate/bbapap

Proteomics of the 26S proteasome in *Spodoptera frugiperda* cells infected with the nucleopolyhedrovirus, AcMNPV

Yulia V. Lyupina [a], Olga G. Zatsepina [b], Marina V. Serebryakova [c], Pavel A. Erokhov [a], Svetlana B. Abaturova [a], Oksana I. Kravchuk [a], Olga V. Orlova [b], Svetlana N. Beljelarskaya [b], Andrey I. Lavrov [d], Olga S. Sokolova [d], Victor S. Mikhailov [a,*]

[a] N.K. Koltzov Institute of Developmental Biology, Russian Academy of Sciences, 26 Vavilova Str., Moscow 119334, Russia
[b] V.A. Engelhardt Institute of Molecular Biology, Russian Academy of Sciences, 32 Vavilova Str., Moscow 119334, Russia
[c] A.N. Belozersky Institute of Physico-Chemical Biology MSU, 1c40 Leninskie Gory, Moscow 119234, Russia
[d] M.V. Lomonosov Moscow State University, Faculty of Biology, 1-12 Leninskie Gory, Moscow 119234, Russia

ARTICLE INFO

Article history:
Received 15 December 2015
Received in revised form 4 February 2016
Accepted 29 February 2016
Available online 3 March 2016

Keywords:
26S proteasome
20S proteasome
Spodoptera frugiperda
Baculovirus
Nucleopolyhedrovirus
AcMNPV

ABSTRACT

Baculoviruses are large DNA viruses that infect insect species such as Lepidoptera and are used in biotechnology for protein production and in agriculture as insecticides against crop pests. Baculoviruses require activity of host proteasomes for efficient reproduction, but how they control the cellular proteome and interact with the ubiquitin proteasome system (UPS) of infected cells remains unknown. In this report, we analyzed possible changes in the subunit composition of 26S proteasomes of the fall armyworm, *Spodoptera frugiperda* (Sf9), cells in the course of infection with the *Autographa californica* multiple nucleopolyhedrovirus (AcMNPV). 26S proteasomes were purified from Sf9 cells by an immune affinity method and subjected to 2D gel electrophoresis followed by MALDI-TOF mass spectrometry and Mascot search in bioinformatics databases. A total of 34 homologues of 26S proteasome subunits of eukaryotic species were identified including 14 subunits of the 20S core particle (7 α and 7 β subunits) and 20 subunits of the 19S regulatory particle (RP). The RP contained homologues of 11 of RPN-type and 6 of RPT-type subunits, 2 deubiquitinating enzymes (UCH-14/UBP6 and UCH-L5/UCH37), and thioredoxin. Similar 2D-gel maps of 26S proteasomes purified from uninfected and AcMNPV-infected cells at 48 hpi confirmed the structural integrity of the 26S proteasome in insect cells during baculovirus infection. However, subtle changes in minor forms of some proteasome subunits were detected. A portion of the α5(zeta) cellular pool that presumably was not associated with the proteasome underwent partial proteolysis at a late stage in infection.

© 2016 Elsevier B.V. All rights reserved.

1. Introduction

The ubiquitin proteasome system (UPS) plays a key role in protection of the cellular proteome from denatured, damaged and toxic proteins. Proteins targeted for digestion are marked with ubiquitin chains typically of three or more ubiquitin moieties by the E1–E2–E3 enzyme cascade and transported to 26S proteasomes for hydrolysis (reviewed in [1]). The 26S proteasome is a multisubunit proteolytic machine of approximately 2.5 MDa with a structure well conserved in evolution and most completely studied in mammals and yeast (reviewed in [2–5]). The 26S proteasome consists of two sub-complexes, the 20S core particle (CP) and the 19S regulatory particle (RP). The CP has a barrel-shaped structure that is composed of four rings of 7 subunits each, two outer rings of α subunits and two internal rings of β subunits (reviewed in [6,7]). Proteolytic activities of proteasomes associated with the catalytic subunits β1, β2, and β5 are caspase-like (also termed peptidyl-glutamyl peptide-hydrolyzing), trypsin-like, and chymotrypsin-like, respectively. The RP confers specificity of binding to ubiquitinated proteins and provides deubiquitination and ATP-dependent protein unfolding. It is composed of the base and lid subcomplexes. The base contains a hetero-hexameric ring of ATPases (RPT1 to RPT6) of the AAA-family and RPN subunits (RPN1 and RPN2) while the lid consists of several non-ATPases (RPNs) and accessory subunits [4,5,8–10]. The lid subunits RPN10 and RPN13 attach to the ubiquitinated substrate, the deubiquitinating enzymes (DUBs) remove the ubiquitin chain, then the base ATPases unfold and translocate the substrate into the 20S CP cavity for hydrolysis. Besides proteolysis of damaged proteins, 26S proteasomes produce immunogenic peptides for presentation by MHC class I system and control many cellular processes including transcription of host and viral genes (reviewed in [11–14]. Isolation of the 26S proteasome from insect species has not been reported, and the function of proteasomes in insect cells remains much less studied than in mammals and yeast.

* Corresponding author.
E-mail address: mikhailov48@mail.ru (V.S. Mikhailov).

http://dx.doi.org/10.1016/j.bbapap.2016.02.021
1570-9639/© 2016 Elsevier B.V. All rights reserved.

The successful evolution of viruses has depended on their ability to avoid the immune response of infected cells and to reprogram the cellular environment for production of viral progeny. Viruses have developed different mechanisms to manage host cell UPS in order to protect proteins essential for their infection cycle from proteolysis by cellular proteasomes. One pathway involves the modification of the host UPS so that it digests cellular antiviral factors. This strategy is used by various RNA and DNA viruses (reviewed in [15–17]) and presumably by baculoviruses. Baculoviruses contain circular double-stranded DNA genomes of 80 to 180 kb and infect insects of the orders Lepidoptera, Hymenoptera, and Diptera (for review see [18]). They encode RING-family ubiquitin ligases [19,20] and require the activity of host cell proteasomes at least at early stages in their infection cycle [21–23]. The proteasome activity in Sf9 cells was decreased during the AcMNPV infection cycle, but the electrophoretic pattern of cellular proteasomes in a native polyacrylamide was unchanged up to 96 hpi [22]. However, the subunit composition of proteasomes in insect cells and possible effects of baculoviruses on the proteasome structure remain undetermined. In this report, we investigated this question by using the model system of the fall armyworm *Spodoptera frugiperda* cells (Sf9) and the most studied baculovirus, *Autographa californica* multiple nucleopolyhedrovirus (AcMNPV).

We describe the purification of the 26S proteasome from Sf9 cells infected with the baculovirus AcMNPV by an immune affinity method. The subunit composition of the 26S proteasome was determined by proteomic analysis that included 2D gel electrophoresis followed by MALDI-TOF mass spectrometry and Mascot search of homologues in bioinformatics databases. Although comparison of 2D-gel maps of 26S proteasomes from uninfected and AcMNPV-infected cells at 48 hpi did not reveal major changes in the proteasome subunit composition, we observed subtle changes in minor forms of some proteasome subunits and partial proteolysis of a cellular pool of α5(zeta) subunits at 48 hpi.

2. Material and methods

2.1. Cells and reagents

S. frugiperda Sf9 cells were cultured in SF-900 II SFM media (Invitrogen) supplemented with 10% fetal bovine serum (FBS) in the flasks at 27 °C. The cells were infected with AcMNPV at a MOI of 10 and incubated for indicated times. Cells were washed with PBS, precipitated by centrifugation and stored at −70 °C. Combined mouse monoclonal antibodies (mAbs) to proteasome α subunits MCP231 were from Enzo Life Sciences. Peroxidase-conjugated anti-mouse IgG and ECL reagents were purchased from GE Healthcare Life Sciences. Fluorogenic proteasome substrates for detection of the chymotrypsin-like and caspase-like activities were Suc-LLVY-AMC (N-Succinyl-Leu-Leu-Val-Tyr-AMC) and Z-LLE-AMC (Z-Leu-Leu-Glu-AMC) from Sigma-Aldrich.

2.2. Purification of the 26S proteasome

Proteasomes were isolated from Sf9 cells using the Rapid 26S Proteasome Purification Kit-S (UBPBio) as described by [24] according to the manufacturer's instructions. Routinely, 10^8 frozen cells were used for purification and resulted in 20 to 25 μg of pure 26S proteasome in 150 μl of a buffer containing 10% glycerol, 40 mM Tris–HCl, pH 7.6, 40 mM NaCl, 2 mM 2-mercaptoethanol, 2 mM ATP, and 5 mM $MgCl_2$. Aliquots of the sample were stored at −70 °C for later analysis.

2.3. Single particle electron microscopy

Glycerol was removed from the 26S proteasome sample by dialysis against a buffer containing 40 mM Tris–HCl, pH 7.6, 40 mM NaCl, 2 mM 2-mercaptoethanol, and 5 mM $MgCl_2$. For EM, 3 μl of the sample was incubated for 30 s on glow-discharged carbon-coated copper grids (400 mesh; Ted Pella, Redding, CA), and then negatively stained with 1% uranyl acetate. Grids were imaged on a JEOL 2100 transmission electron microscope (JEOL), operating at 200 kV. Images of proteasomes were captured using Ultrascan 1000XP CCD (Gatan) at 40,000× magnification and 1.5–1.8 μm underfocus. Particles were selected from the EM images using Boxer [25] and windowed into 200 × 200 pixel images. These were then filtered and normalized to a standard deviation of 1, and processed for reference-free classification in IMAGIC [26], that yielded 20 classes. Representative class-sum images are presented in Fig. 1C.

2.4. MALDI-TOF mass spectrometry

Mass spectra of the tryptic peptides of Sf9 proteins were obtained by using the matrix-assisted laser desorption/ionization (MALDI) time-of-flight mass (TOF) spectrometer Ultraflextreme BRUKER (Germany), equipped with UV laser (Nd) and reflectron. Briefly, proteins of interest in pieces (2 × 2 mm) from a 2D polyacrylamide gel were washed twice in 100 μl 40% acetonitrile in 0.1 M NH4HCO3, once in 100 μl of acetonitrile and were hydrolyzed with 4 μl of the modified trypsin (Promega) (15 μg/ml in 0.05 M NH4HCO3) at 37°C for 18 h. After mixing with 7 μl 0.5% trifluoroacetic acid (TFA), portion of 0.5 μl from the sample was mixed with 0.5 μl 2,5-dihydroxy benzoic acid (Aldrich), 20 mg/ml in 30 % acetonitrile and 0.5% TFA, spotted on a MALDI plate and air dried. The monoisotopic mass of the tryptic peptides as positive ions was measured with an accuracy of 30 ppm. The spectra of peptide fragmentation were obtained in the Lift mode with the accuracy of 1Da for daughter ions. Identification of Sf9 proteins was performed by using Mascot software (www.matrixscience.com) in the NCBI database and database of invertebrates EST taking into account possible oxidation of methionines and modification of cysteines by acrylamide.

2.5. Other methods

Electrophoresis in a native polyacrylamide gel followed by detection of proteasome activity in the gel was performed as described earlier [22]. Two-dimensional PAGE was carried out by the method of O'Farrell [27] as previously described [28]. SDS-polyacrylamide gel electrophoresis (PAGE) was performed as described [29]. For Western blotting, proteins were transferred on Hybond-ECL membrane (Amersham) and probed with mAb MCP231.

3. Results

Fractionation of Sf9 extracts in a native polyacrylamide gel revealed three proteasome bands marked by arrows in Fig. 1A and associated with the chymotrypsin-like (1) and caspase-like (lane 2) activities. Western blotting and probing with monoclonal antibodies to α-subunits confirmed the presence of distinct proteasome complexes in each of the bands (lane 3). These bands were tentatively identified as the core particles (CP, 20S proteasome), complexes of CP with proteasome activators (PA), and CP combined with 19 S regulatory particle (RP) according to the electrophoretic pattern of mammalian proteasomes (lane 4) described by others [30,31]. The 20S proteasome is known to hydrolyze predominantly proteins without conjugated ubiquitin, whereas the CP–RP complex (26S proteasome) digests the polyubiquitinated proteins and is responsible for fine tuning of the cellular proteome [5,6]). We applied the proteomic methods to characterize the 26S proteasomes from uninfected or AcMNPV-infected *S. frugiperda* (Sf9) cells.

A kit supplied by UBPBio was used to purify 26S proteasomes from extracts of Sf9 cells. The high-speed supernatants (Sup) of cellular lysates retained activities of all proteasome forms (Fig. 1B, lane 1). The CP–RP and CP proteasome fractions were revealed after the native electrophoresis of the purified 26S sample (Prot) (lane 2). Western blotting and probing with antibodies to α-subunits confirmed the presence of CP complexes with the proteasome activators in the supernatants

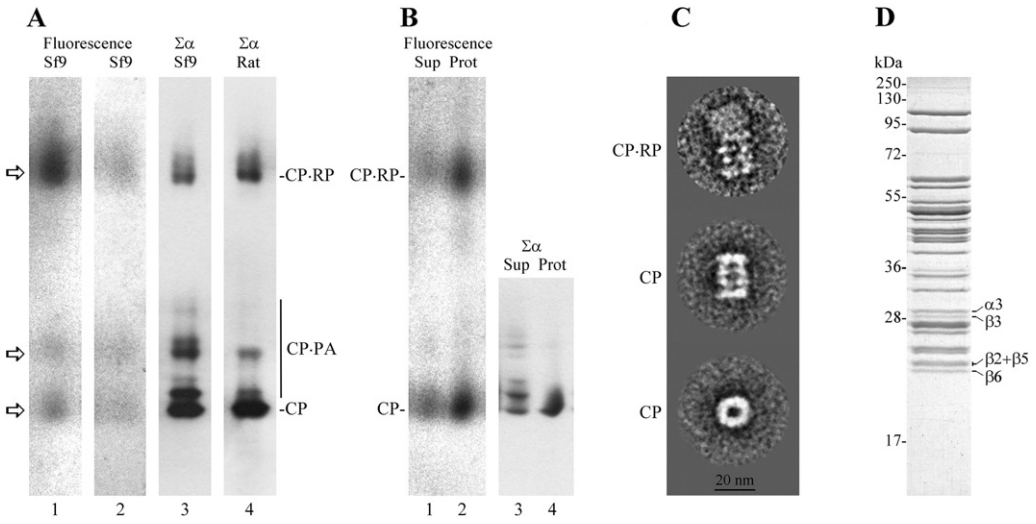

Fig. 1. Characterization of *Spodoptera frugiperda* proteasomes by polyacrylamide gel electrophoresis and electron microscopy. (A) Electrophoresis of cell extracts in a native gel under nondenaturing conditions. Chymotrypsin-like (lane 1) and caspase-like (lane 2) activities in the gel. Extracts from S9 cells (lane 3) and from rat liver cells (lane 4) after Western blotting and probing with mAb to proteasome α-type subunits. (B) Electrophoretic pattern of proteasomes from high-speed supernatant (Sup, lanes 1 and 3) and from purified 26S sample (Prot, lanes 2 and 4) in a native gel. Chymotrypsin-like activity in the gel (lanes 1 and 2). Lanes 3 and 4 show the lanes 1 and 2 (parts with core particles) after Western blotting and probing with mAb to proteasome α-type subunits. (C) Electron microscopy images of 26S (filtered one particle) and 20S (sum of filtered and aligned 10 particles) proteasomes in the sample purified from Sf9 cells. Sidewise view (upper panels) and bottom view (down panel) are shown. (D) Fractionation of purified 26S proteasomes by SDS-13% PAGE followed by Coomassie staining. The marked bands were cut from the gel and identified by using MALDI-TOF mass spectrometry and Mascot software as proteasome subunits of α-and β-type. CP — core particle; RP — regulatory particle; PA — proteasome activator.

(lane 3). However, the purified sample (Prot) was almost free of these extra CP-forms (lane 4). Because the purification method utilizes the affinity bait (GST–Ubl) specific for 26S proteasomes, the appearance of pure CP in the 26S sample reflects presumably partial dissociation of the CP–RP complex that usually resulted from its electrophoresis in polyacrylamide gels, as well as from storage and handling. CP associated with one RP and free CP were the predominant proteasome complex in the purified samples and showed typical structures of 26S and 20S proteasomes under visualization by single particle electron microscopy (Fig. 1C). SDS-PAGE analysis of the purified sample showed pattern typical for the 26S proteasome with dozens of protein bands ranging from approximately 20 to 110 kDa (Fig. 1D). Four bands were cut from the gel, digested with trypsin and analyzed by MALDI-TOF mass spectrometry followed by Mascot search for homologous proteins in the Invertebrates_EST EST and NCBInr database (data not shown). These proteins were unambiguously identified as the proteasome subunits α3, β3, and β6 and a mixture of β2 and β5. Next we used a standard proteomic procedure along with 2D gel electrophoresis to increase the resolution capacity and to characterize the subunit composition of 26S proteasomes from Sf9 cells.

2D electrophoresis of 26S proteasomes purified from Sf9 cells was carried out by electrofocusing in polyacrylamide in a range of approximately 4.5 to 8.5 pH in the first direction followed by SDS-13% PAGE in the second direction. A typical protein pattern obtained is shown in Fig. 2A. Basic proteins of 26S proteasomes were also fractionated by 1D electrofocusing in a range of 8.0 to 10.0 pH (Fig. 2B). A total of 50 bands stained with Coomassie were recognized; these bands were cut from the gels and subjected to mass spectrometry followed by Mascot search. Results of the *in silico* analysis are shown in Table 1. Homologues with the highest scores and some of selected species are shown for each band. From the total number of 50, 47 protein bands were confirmed to represent the proteasome subunits. 34 protein bands were identified by a direct search in the NCNInr database, 10 bands were first identified in the Invertebrates_EST EST database and then by using NCBI/BLAST/blastx. One spot (#45) was identified by MS/MS search. Two proteins (##41, 43) in the sample did not reflect structural components of proteasomes and appeared presumably due to the purification method. Protein #41 was the affinity bait GST–Ubl added to the sample for purification and not completely removed, whereas a minor protein band #43 was the host cell glutathione S-transferase retained on the glutathione sepharose resin that was used to bind the GST–Ubl-26S proteasome complex. Protein #42 showed the highest homology to *Escherichia coli* DnaK chaperone, thus it might contaminate the kit components or represent an unknown chaperone of the HSP70 family in Sf9 cells. Bands ##49 and 50 showed scores below the significant threshold but both contained peptides R.GAQLYYVDSEGTR.T (1458.7) and R.YQGGVLLAVDSR.A (1277.7), that were detected in the trypsin digest of protein #48 and in β5 subunits of different insects. We concluded that ##49 and 50 might represent subforms of the β5 subunit.

Some 47 proteins in the gels shown in Fig. 2A,B present in total 20 homologues of the yeast proteasome 19S RP subunits — 11 of RPN-type, 6 of RPT-type and 3 accessory subunits (ubiquitin hydrolases UCH-14/UBP6 and UCH-L5/UCH37, thioredoxin TRX). Two sets of α- and β-subunits each of 7 composed a full structure of CP, 20S proteasome. Subunits 1 (RPN2) and 2 (RPN1) combined with 6 ATPase regulatory subunits of RPT-type (4A, 6B, 6A, 7A-7B, 10B, and 8T) formed a base of RP. 9 subunits of RPN-type (4B, ARDM1, 12, 11, 6N, 13, 7N, 14, 8N) with the accessory factors UCH-14/UBP6, UCH-L5/UCH37, and TRX composed a lid of RP. Three subunits (14/RPN11, UCH-14/UBP6, and UCH-L5/UCH37) serve as deubiquitinating enzymes (DUBs). The RP assembly contains all factors required for binding ubiquitinated proteins (RPN13 and RPN10), removing of the ubiquitin moieties (RPN11, UCH-14/UBP6, and UCH-L5/UCH37) and ATP-dependent processing of folded proteins (6 RPTs). The presence of thioredoxin (TRX) among structural subunits allows to process proteins containing disulfide bonds. The 26S proteasome samples purified from Sf9 cells possessed proteolytic activity (Fig. 1B, lane 2). All these data suggest that the samples present functional proteasomes and the 2D map shown in Fig. 2 reflects a true composition of 26S proteasomes in *Spodoptera* cells. The gels revealed also structural varieties in the 26S proteasome pool. Several subunits provided two separate spots in the gels such as Sub. 1 (RPN2) — spots ##1 and 2; Sub.7 (RPT1) — ##10 and 11; Sub. 10B (RPT4) — ##14 and 15; Sub. 13 (RPN9) — ##17 and 18; Sub. 14 — ##22 and 24; and β7 — ##30 and 33. In some cases the subunits showed a minor band in addition to the major fraction as that the Sub. 1 (##1, 2) and Sub. 14 (##22, 24), whereas other duplets such as

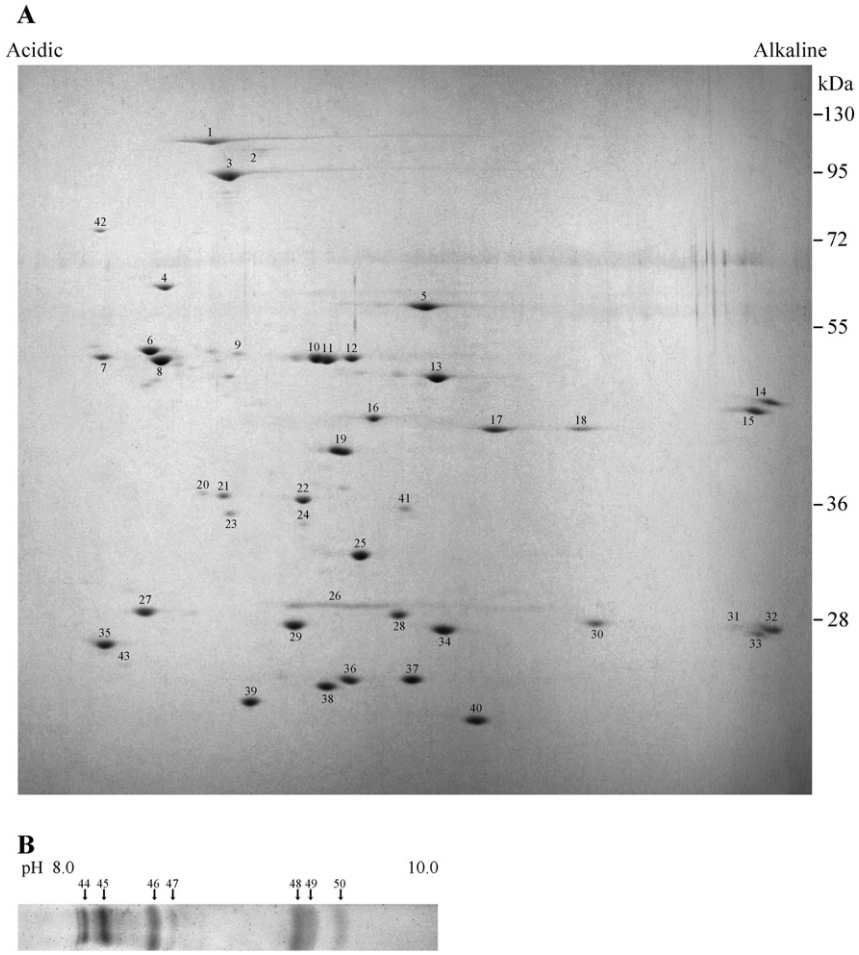

Fig. 2. (A) Fractionation of 26S proteasomes purified from Sf9 cells by 2D electrophoresis. The first direction was electrofocusing in the pH range from 5 to 8.5. The second direction was SDS-13% PAGE followed by Coomassie staining. The stained bands numbered 1 to 43 from the gel top were cut from the gel and identified by using MALDI-TOF mass spectrometry and Mascot software. (B) Basic proteins from the purified 26S proteasomes were fractionated by electrofocusing in a 5% polyacrylamide gel in a pH range from 8 to 10 followed by Coomassie staining. The stained bands numbered 44 to 50 were extracted from the gel and identified as above.

Sub.7 (##10, 11) and β7 (##30, 33) showed splitting in two comparable bands. Interestingly, factors involved in binding and processing of ubiquitinated proteins, RPN13, UCH-14/UBP6, UCH-L5/UCH37, and TRX, were present in lower molar amounts than other subunits of RP and CP particles according to the Coomassie staining of 2D gels. It suggests structural heterogeneity of RPs in the purified 26S proteasome samples. Homologues of RPN3 and Sem1/DSS1 were not found among the identified Lid subunits. The proposed *rpn3* gene in *Bombyx mori* genome (accession XP_004931019) encodes protein of 56.2 kDa. We did not recognize any protein band of respective molecular mass in the 2D gel after Coomassie staining except spot #4 that associated with UCH-14 hydrolase (Fig. 2A). Overstaining of the gels with silver also did not reveal any promising candidate for RPN3 (data not shown). A small acidic subunit Sem1/DSS1 (app. 89 amino acid residues) was also not identified in the purified samples.

The Sf9 proteasome subunit β5 showed an unexpected migration pattern upon the SDS-PAGE analysis and isoelectric focusing. It behaved like a protein with a molecular mass of 23 kDa (Fig. 1D) and pI value of about 9 (Fig. 2B, spots ##48–50). However, the homologous β5 subunits in insect species *Plutella xylostella* and *B. mori* (Table 1) have molecular masses of approximately 31 kDa and pI values of 5.6 and 6.1 respectively. This suggested that the β5 subunit in Sf9 cells might be processed to a shorter form with an alkaline pI as shown previously for mammalian cells [32,33]. The ESTs in spodobase (bioweb.ensam.inra.fr/spodobase/) did not allow reconstruction of a Sf9 proteasome β5 gene. However, the subunit β5 of a closely related species, *Spodoptera exigua*, was obtained from EST Se1E13636-5-1. The protein is composed of 281 amino acids and has a molecular mass of 30,774.80 and pI value of 6.7. These values are close to those predicted for the insect species mentioned above. Alignment β5 subunits of *S. exigua* (Se β5) and Human (P28074|PSB5) by using CLUSTALW (1.2.1.) multiple sequence alignment software showed a high level of identity (52.6%) especially in the C-terminal part (see below).

```
Se β5          1 MALLDFCQLDQKINLKPVDALASFENDVVGY--SG--NFLHSTHLATPPF  46
                 || |: ..|: : .| ||:. .:|      :  :|  ::|   :|:::::
P28074|PSB5    1 ma-la-svle-r-pl-pvnq-rgf------fglggradll---dlgpgsl  35

Se β5         47 ANPVETL-AQ-FNQKDETGKAIKIQFDHGTTTLGFRYQGGVLLAVDSRAT  94
                 :::: :| |: ::..:|:|  |:: : ||||||:|:::.||::|.|||||
P28074|PSB5   36 sdgl-slaapgwgvpeepg--iem-l-hgtttlafkfrhgvivaadsrat  80

Se β5         95 GGQFIGSQSMKKIVEINDYLLGTLAGGAADCVYWDRVLAKQCRLYELRNR  144
                 :|.:|:||::|:::|||.|||||:|||||||.:|:|:||:|||:|||||:
P28074|PSB5   81 agayiasqtvkkvieinpyllgtmaggaadcsfwerllarqcriyelrnk  130

Se β5        145 ERISVAAASKLMANMVYNYKGMGLSMGMMLAGV-DKRGAQLYYVDSEGTR  193
                 ||||||||||:|||||:|||||||||.|:.|  ||||:.||||||||.|
P28074|PSB5  131 erisvaaaskllanmvyqykgmglsmgtmicg-wdkrgpglyyvdsegnr  179

Se β5        194 TPGKVFSVGSGSVYAFGVLDSGYSWDLSD-KDAQ-ELGRRAIYHATHRDA  241
                 .:|..||||||||||:||:|.|||:|| : ::|  :|:||||||:||.|||
P28074|PSB5  180 isgatfsvgsgsvyaygvmdrgysydl-eveqa-ydlarraiyqatyrda  227

Se β5        242 YSGGIVRVYHISEKGWVNISNEDCSDLHY-KYAAEKGNVGA    281
                 ||||.|::||:.|:||:::|:::.:|||  ||:::.:
P28074|PSB5  228 ysggavnlyhvredgwirvssdnvadlh-ekysgstp----    263
```

Table 1
26S proteasome subunits of *Spodoptera frugiperda* Sf9 cells identified by *in silico* analysis using Mascot software and bioinformatics databases.

Spot no.	Reference	Accession		Mass	No. of peptides[a]	E-value[b]	Putative protein	Yeast homologue
1	Sub. 1	GI:512914524	XP_004928163	109758	16	0.00019	26S proteasome non-ATPase regulatory subunit 1-like [*Bombyx mori*]	RPN2
2	Sub. 1	GI:512914524	XP_004928163	109758	18	7.3e−06	26S proteasome non-ATPase regulatory subunit 1-like [*Bombyx mori*]	RPN2
3	Sub. 2	GI:512931070	XP_004932217	101718	18	3e−07	26S proteasome non-ATPase regulatory subunit 2-like [*Bombyx mori*]	RPN1
4	UCH-14	GI:300757465	FQ015829	55103	11	0.042	Spodoptera littoralis, EST, male antenna	UBP6
			XP_004927226			3e−146	Ubiquitin carboxyl-terminal hydrolase 14-like [*Bombyx mori*]	
5	Sub. 4A	GI:389611682	BAM19425	49539	21	3e−19	Proteasome 26S subunit 4 ATPase, partial [*Papilio xuthus*]	RPT2
		GI:512899104	XP_004924561	44127	21	1.5e−16	26S protease regulatory subunit 4-like, partial [*Bombyx mori*]	
6	Sub. 6B	GI:389609377	BAM18300	41782	31	3.8e−29	26S protease regulatory subunit rpt3 [*Papilio xuthus*]	RPT3
		GI:114053311	NP_001040338	47053	28	7.6e−24	26S protease regulatory subunit 6B [*Bombyx mori*]	
7	Sub. 4B	GI:148298816	NP_001091810	39272	6	7.6e−14	Proteasome 26S non-ATPase subunit 4 [*Bombyx mori*]	RPN10
8	Sub. 6A	GI:357613322	EHJ68433	47651	30	1.5e−23	26S protease regulatory subunit 6A [*Danaus plexippus*]	RPT5
		GI:512894321	XP_004923401	51453	28	3.8e−20	26S protease regulatory subunit 6A-like [*Bombyx mori*]	
9	ARDM1	GI:357618033	EHJ71129	41099	9	1.9e−12	Hypothetical protein KGM_08118 [*Danaus plexippus*] (proteasomal ubiquitin receptor ADRM1-like protein)	RPN13
10	Sub. 7A	GI:512896702	XP_004923974	48564	24	2.4e−13	26S protease regulatory subunit 7-like isoform X1 [*Bombyx mori*]	PRT1
		GI:389609441	BAM18332	48494	22	1.5e−09	26S protease regulatory subunit rpt1 [*Papilio xuthus*]	
11	Sub. 7B	GI:389609441	BAM18332	48494	31	2.4e−22	26S protease regulatory subunit rpt1 [*Papilio xuthus*]	RPT1
		GI:512896702	XP_004923974	48564	29	7.6e−20	26S protease regulatory subunit 7-like isoform X1 [*Bombyx mori*]	
12	Sub. 12	GI:389610877	BAM19049	50770	16	9.6e−08	Proteasome regulatory subunits rpn5 [*Papilio polytes*]	RPN5
		GI:357606923	EHJ65283	46320	14	9.6e−05	Proteasome 26S non-ATPase subunit 12 [*Danaus plexippus*]	
		GI:114052086	NP_001040208	51782	12	0.058	Proteasome 26S non-ATPase subunit 12 [*Bombyx mori*]	
13	Sub. 11	GI:357609221	EHJ66352	47095	22	7.6e−14	Hypothetical protein KGM_03290 [Danaus plexippus]	RPN6
		GI:512901637	XP_004925184	47219	19	1.9e−09	26S proteasome non-ATPase regulatory subunit 11-like [*Bombyx mori*]	
14	Sub. 10B	GI:114052605	NP_001040484	44749	9	0.00011	26S proteasome regulatory ATPase subunit 10B [*Bombyx mori*]	RPT4
15	Sub. 10B	GI:2960216	CAA11285	44579	19	1.1e−17	26S proteasome regulatory ATPase subunit 10B [*Bombyx mori*]	RPT4
16	Sub. 6N	GI:512926210	XP_004931028	43434	12	9.6e−07	26S proteasome non-ATPase regulatory subunit 6-like [*Bombyx mori*]	RPN7
		GI:389614706	BAM20379	33802	10	3.8e−05	26S proteasome non-ATPase regulatory subunit rpn7, partial [Papilio polytes]	
17	Sub. 13	GI:300756460	FQ015686		10	1.9e−05	*Spodoptera littoralis*, EST, male antenna	RPN9
			BAM20039	41099		2e−148	26S proteasome subunit rpn9 [*Papilio xuthus*]	
			NP_001040331	42884		7e−142	26S proteasome non-ATPase regulatory subunit 13 [*Bombyx mori*]	
18	Sub. 13	GI:389613367	BAM20039	41099	3	3.7e−07	26S proteasome subunit rpn9, partial [*Papilio xuthus*]	RPN9
19	Sub. 7N	GI:357609699	EHJ66586	34068	12	1.5e−12	Proteasome 26S non-ATPase subunit 7 [*Danaus plexippus*]	RPN8
		GI:114052713	NP_001040543	37472	11	7.6e−10	Proteasome 26S non-ATPase subunit 7 [*Bombyx mori*]	
20	UCH L5	GI: 300746376	FQ030615		5	2.5e−05	Spodoptera littoralis, EST, male antenna	UCH37
			EHJ66626	37370		1e−145	Hypothetical protein KGM_08817 [*Danaus plexippus*]	
			XP_004933129	42766		2e−137	Ubiquitin carboxyl-terminal hydrolase isozyme L5-like isoform X2 [*B. mori*]	
21	UCH L5	GI: 300746446	FQ030660		14	2.4e−09	Spodoptera littoralis, EST, male antenna	UCH37
			EHJ66626	37370		3e−161	Hypothetical protein KGM_08817 [*Danaus plexippus*]	
			XP_004933129	42766		9e−149	Ubiquitin carboxyl-terminal hydrolase isozyme L5-like isoform X2 [*B. mori*]	
22	Sub. 14	GI:357609599	EHJ66532	34541	11	0.00012	26S proteasome non-ATPase regulatory subunit 14 [*Danaus plexippus*]	RPN11
		GI:114052633	NP_001040263	34547			26S proteasome non-ATPase regulatory subunit 14 [*Bombyx mori*]	
23	TRX	GI: 399121912	JK788365		8	0.0077	*Spodoptera exigua* cDNA	
			EHJ72116	31510		4e−178	Thioredoxin [*Danaus plexippus*]	
			NP_001040348	31747		7e−171	Thioredoxin [*Bombyx mori*]	
24	Sub. 14	GI:357609599	EHJ66532	34541	11	0.00037	26S proteasome non-ATPase regulatory subunit 14 [*Danaus plexippus*]	RPN11
25	α1	GI:512891246	XP_004922650	30377	10	0.00012	Proteasome subunit alpha type-1-like [*Bombyx mori*]	α1
26	α3	GI:114051245	NP_001040387	28240	8	1.2e−05	Proteasome alpha 3 subunit [*Bombyx mori*]	α3
27	β3	GI:114052162	NP_001040460	23045	6	1.2e−14	Proteasome beta 3 subunit [*Bombyx mori*]	β3
28	Sub. 8N	GI: 399551144	FQ976349		10	3.8e−11	Spodoptera littoralis cDNA library, female antennal cDNA	RPN12
			BAM18345	30250		5e−151	26S proteasome non-ATPase regulatory subunit rpn12 [Papilio xuthus]	
			XP_004925604	30578		3e−146	26S proteasome non-ATPase regulatory subunit 8-like [*Bombyx mori*]	
29	α4	GI:357603122	EHJ63634	28722	9	9.6e−06	Proteasome alpha 4 subunit [*Danaus plexippus*]	α4
30	β7	GI:357604314	EHJ64129	29474	4	3.7e−21	Proteasome subunit beta 7 [*Danaus plexippus*]	β7
		GI:114053073	NP_001040536	30549	4	4.6e−21	Proteasome subunit beta 7 [*Bombyx mori*]	
31	α7	GI:114052034	NP_001040204	27855	5	7.3e−14	Proteasome beta-subunit [*Bombyx mori*]	α7
		GI:189237685	XP_969117	28067	5	7.3e−14	Proteasome subunit alpha type-7-1 [*Tribolium castaneum*]	
32	α7	GI:114052034	NP_001040204	27855	8	0.00091	Proteasome beta-subunit [*Bombyx mori*]	α7
		GI:189237685	XP_969117	28067	8	0.00091	Proteasome subunit alpha type-7-1 [*Tribolium castaneum*]	
33	β7	GI:357604314	EHJ64129	29474	7	0.018	Proteasome subunit beta 7 [*Danaus plexippus*]	β7
34	α6	GI:114052160	NP_001040459	27126	9	0.00038	Proteasome subunit alpha type 6-A [*Bombyx mori*]	α6
35	α5 (zeta)	GI:357625487	EHJ75913	29750	11	2.4e−06	Proteasome zeta subunit [*Danaus plexippus*]	α5 (zeta)
		GI:114050993	NP_001040146	26857	9	0.014	Proteasome zeta subunit [*Bombyx mori*]	
36	β1	GI:211939905	ACJ13433	25525	12	1.9e−09	Proteasome subunit beta 1 [*Helicoverpa armigera*]	β1
37	β4	GI: 90137213	DY792998		16	1.2e−14	*Spodoptera frugiperda* cDNA	β4
			XP_004933282	28744		3e−124	Proteasome subunit beta type-4-like [*Bombyx mori*]	
38	α2	GI:357622706	EHJ74121	25766	16	3e−14	Proteasome 25 kDa subunit [*Danaus plexippus*]	α2
		GI:114052504	NP_001040344	25808	13	7.6e−08	Proteasome 25 kDa subunit [*Bombyx mori*]	
39	β2	GI: 295258532	FP350589		8	1.9e−06	Sf2H02408–5-1, *Spodoptera frugiperda* (fall armyworm), EST	β2
			EHJ75038	23140		3e−128	Hypothetical protein KGM_19166 [*Danaus plexippus*]	
			XP_004928268	22952		7e−126	Proteasome subunit beta type-2-like isoform X1 [*Bombyx mori*]	
40	β6	GI:295291143	FP375344		9	9.7e−05	Sf2M08476–3-1, *Spodoptera frugiperda* (fall armyworm), EST	β6
			EHJ65339	22330		2e−125	Hypothetical protein KGM_11399 [*Danaus plexippus*]	

Table 1 (*continued*)

Spot no.	Reference	Accession		Mass	No. of peptides[a]	E-value[b]	Putative protein	Yeast homologue
			XP_004923023	24029		4e−123	Proteasome subunit beta type-6-like [*Bombyx mori*]	
41	GST–Ub	GI:62738608+	GI:46015810			7.6e−11	Fusion of GST with the Ub-like domain of RAD23B	
42	DnaK	GI:446438283	WP_000516138	67286	16	1.1e−13	Chaperone protein DnaK [*Escherichia coli*]	
		GI:498977694	XP_004528661	134459	15	3.1e−06	Chaperone protein DnaK-like [*Ceratitis capitata*]	
43	GST	GI:295275715	FP368242		6	0.0012	Sf1P01988-5-1, *Spodoptera frugiperda* (fall armyworm)	
			AIH07591	23090		2e−136	Glutathione S-transferase sigma 4 [*Spodoptera litura*]	
44	Sub. 10B	GI:114052605	NP_001040484	44749	13	1.8e−08	26S proteasome regulatory ATPase subunit 10B [*Bombyx mori*]	RPT4
45	α7	GI:114052034	NP_001040204	27855		3e−10	Proteasome beta-subunit [*Bombyx mori*]	α7
		GI:189237685	XP_969117	28067		3e−10	Proteasome subunit alpha type-7-1 [*Tribolium castaneum*]	
46	Sub. 8T	GI:1709799	P54814	45309	24	5.7e−13	RecName: Full = 26S protease regulatory subunit [*Manduca sexta*]	RPT6
		GI:512906261	XP_004926152	45422	23	1.4e−11	Predicted: 26 protease regulatory subunit 8 [*Bombyx mori*]	
47	Sub. 8T	GI:1709799	P54814	45309	15	1.8e−10	RecName: Full = 26S protease regulatory subunit [*Manduca sexta*]	RPT6
		GI:512906261	XP_004926152	45422	15	2.2e−10	Predicted: 26 protease regulatory subunit 8 [*Bombyx mori*]	
48	β5	GI: 768424547	XP_011553233	30921	7	7.1e−21	Predicted: proteasome subunit beta type-5 [*Plutella xylostella*]	β5
		GI:512890860	XP_004922586	31298	5	5.6e−07	Predicted: proteasome subunit beta type-5 [*Bombyx mori*]	

Search was performed in database NCBInr; spots ##4, 17, 20, 21, 23, 28, 37, 39, 40, and 43 were analyzed first in database Invertebrates_EST EST and then by using NCBI/BLAST/blastx. Spot #45 was analyzed by MS/MS search. All shown scores were significant ($p < 0.05$).

[a] This is the number of peptide sequences identified by Mascot that contributed to the protein score.

[b] *E*-values generated by Mascot.

Remarkably, the Se β5 contains motif 72-HGTTTL-77 which serves as the processing site for the production of a mature form of the mammalian β5 subunit with TTTL at the N-terminus. Deletion of the proposed N-terminal propeptide (1–73 aa) in the *S. exigua* β5 should generate a catalytically active group TTTL at the N-terminus and a protein having a molecular mass of 22.7 kDa and pI value of 8.7, which is very close to the values shown by the *S. frugiperda* β5 subunit under electrophoresis (Figs. 1D and 2B). The data we obtained suggest that processing of the subunit β5 in insect cells proceeds in the same manner as in mammalian cells thus producing functional subunit β5 with a lower molecular mass and alkaline pI.

In order to elucidate possible proteasome modifications in Sf9 cells during the course of baculovirus infection, we directly compared the subunit patterns in 2D gels of 26S proteasomes purified from uninfected and AcMNPV-infected cells at 48 hpi. This analysis revealed that the position of major and minor forms of the proteasome subunits in 2D gels and their quantitative prevalence was not changed due to the virus infection. Selected portions of the gels with RP and CP subunits of 26S proteasomes purified from the uninfected and infected cells are shown in Figs. 3 and 4. Attribution of all marked bands in the figures referenced according to the subunit ID in Table 1 was confirmed by mass spectrometry and Mascot search. The figures provide additional information about minor forms of proteasome subunits. Interestingly, subunit ARDM1 (RPN13 homologue) was comprised of three minor forms (marked by "A" in Fig. 3). This subunit together with RPN10 (Sub. 4B) serves as an intrinsic ubiquitin receptor [8], and its heterogeneity suggests specificity in interaction with different ubiquitin chains. RPN13 presumably interacts with the ubiquitin carboxyl-terminal hydrolase UCH-L5/UCH37 (##20, 21 in Fig. 2A) [34,35]. Two other DUBs, UCH-14/UBP6 (#4) and RPN11 (###22, 24), interact respectively with base subunits, RPN1 and RPT1 [36] and with lid subunits (RPN9 and RPN5) [8]. Appearance of minor subunit forms with lower molecular masses in gels suggests partial proteolysis from one or both ends. The subunit 6B is encoded in *Spodoptera* cells by EST Sf1F09464-3-1 (bioweb.ensam.inra.fr/spodobase/) and contained the C-terminal peptide KKDESEYEFYK (1137.61). This fragment was identified in trypsin digests of three minor forms of 6B indicating that these forms were presumably produced by limited hydrolysis from N-terminus of Sub. 6B. Absence of annotated gene sequences for many proteasome subunits in *Spodoptera* cells precludes further analysis of chemical modifications of minor forms. Fig. 4 shows the 2D patterns of 11 subunits of CP and 1 subunit of RP (8N). Several minor forms (β3a, β1a, α1a, 8Na and β7a) were also identified in the samples as well as traces of host cell glutathione-S-transferase (GST). Distal alkaline portions of the 2D gels did not reveal difference in patterns of subunits α7 and β7 (spots ##31, 32, and 33 in Fig. 2A) between uninfected and infected cells (data not shown). The pattern of the α3 subunit from both uninfected and infected cells was rather unusual displaying a broad distribution in pI. The subunit is encoded by Sf9L05754-Contig1 (bioweb.ensam.inra.fr/spodobase/). Trypsin digest of the left and right portions of α3 band revealed only internal fragments of this protein, and the cause for its broad distribution in the gel is unclear. The comparison of 26S proteasomes from uninfected and AcMNPV-infected Sf9 cells confirmed that the virus infection did not affect the general subunit composition of 26S proteasomes. This conclusion was in agreement with the unchanged proteasome pattern in a native gel during AcMNPV-infection cycle observed in earlier paper [22]. However, subtle changes in minor forms of some proteasome subunits (β3a, β1a, α1a, 8Na, and β7a) were detected and deserve further analysis.

Monoclonal mouse antibodies MCP231 (Enzo Life Sciences) allowed direct analysis of α-subunits in crude extracts of Sf9 cells by Western blotting [22]. In subsequent experiments, uninfected and AcMNPV-infected cell lysates at 24 and 48 hpi were subjected to the 2D electrophoresis followed by Western blotting with mAb MCP231 (Fig. 5). Six immunoreactive protein bands were identified as α-subunits 1 to 6 according to their position in gels and previous mass spectrometry identification (Figs. 2A and 4, Table 1). One subunit, α3, showed a band shifted to the acidic side of the gel and more condensed than respective bands from the purified 26S proteasome samples (compare with Fig. 4). Meanwhile the position of α3 protein from the cellular extracts in 2D gels was not affected by the virus infection (Fig. 5). The different positions of the α3 band in the purified 26S proteasome and in crude

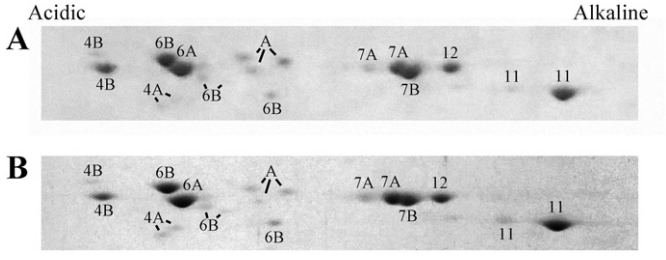

Fig. 3. RP subunits from the 26S proteasomes purified from uninfected Sf9 cells (A) and from cells infected with AcMNPV at a MOI of 10 and collected at 48 hpi (B). Portions of the stained 2D gels show proteins in a range approximately 46 to 55 kDa. The proteins are marked by the subunit numbers given in Table 1 (A — ARDM1).

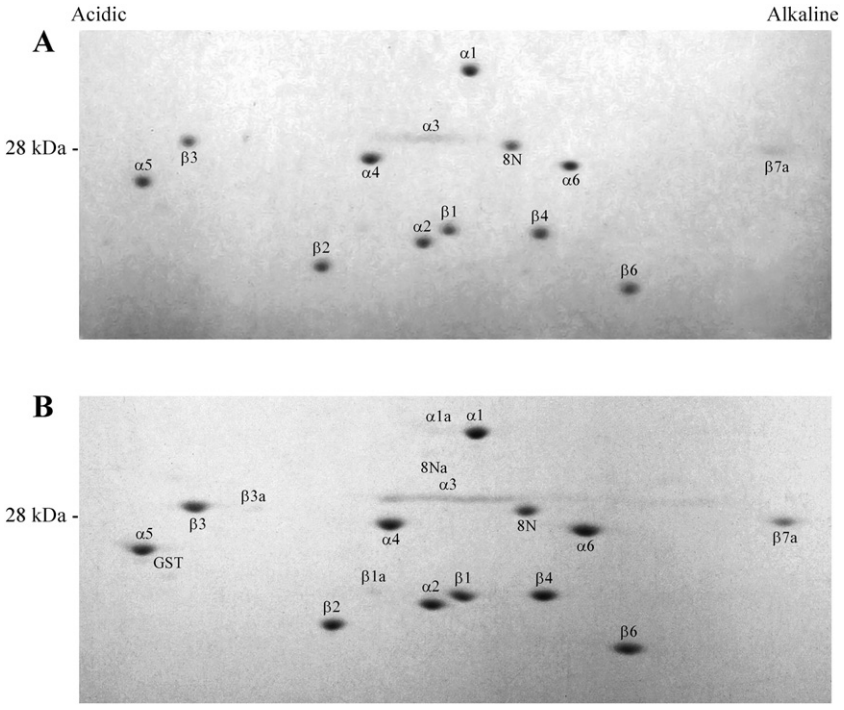

Fig. 4. CP subunits from the 26S proteasomes purified from Sf9 cells uninfected (A) and infected with AcMNPV at a MOI of 10 and collected at 48 hpi (B). Portions of the stained 2D gels show proteins in a range approximately 22 to 34 kDa. GST — glutathione-S-transferase.

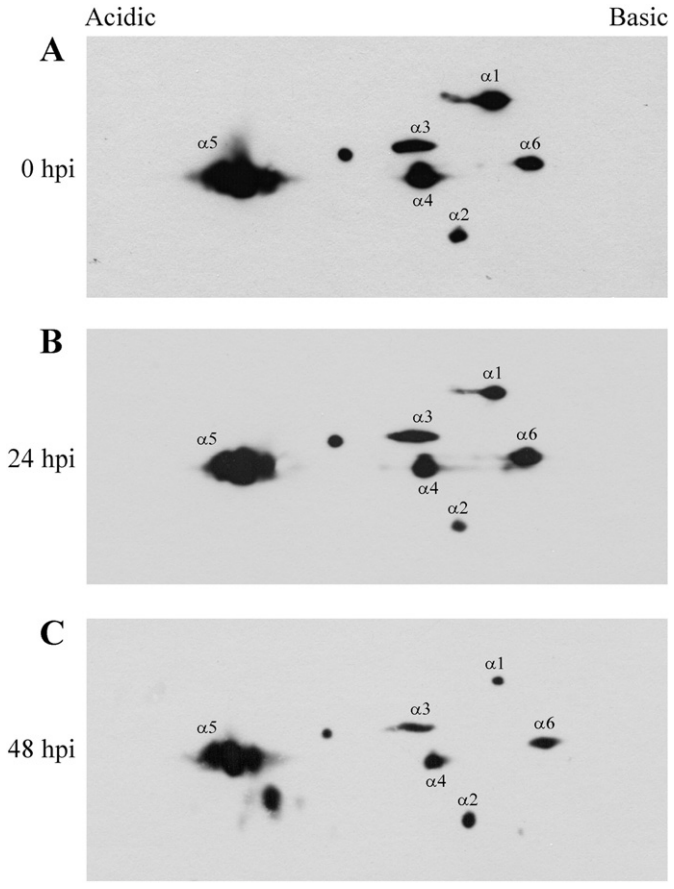

Fig. 5. Proteasome α-type subunits in Sf9 cells uninfected (A) and infected with AcMNPV at a MOI of 10 and collected at 24 hpi (B) and 48 hpi (C). The cell extracts were fractionated by 2D electrophoresis with electrofocusing in the first direction and by SDS-13% PAGE in the second direction followed by Western blotting and probing with mAb to proteasome α-type subunits.

extracts might reflect difference in cellular subfractions of α3 or chemical modification of the α3 subunit under 26S proteasome purification that resulted in the shifted and broad band in the 2D gels. Another subunit, α5(zeta), provided adjacent overlapping bands under analysis of crude extracts that were clearly distinct from the uniform band in the purified 26S proteasomes (Fig. 4) and showed partial proteolysis at 48 hpi. Because the α5(zeta) subunit showed an identical band pattern in the proteasome samples purified from uninfected and AcMNPV-infected cells (Fig. 4), partial proteolysis of the cellular α5(zeta) pool at 48 hpi might reflect selective processing of the α5(zeta) fraction that was not associated with the proteasome. The proteasome subunit α5(zeta) might possess a ribonuclease activity, and in mammalian cells a large portion of the α5(zeta) cellular pool is not associated with proteasomes and persists as a free monomer in both nuclei and cytoplasm [37]. The free monomer does not exchange with α5(zeta) in proteasomes and has a turnover rate much higher than the α5(zeta) associated with proteasome [37]. Our data suggest that the free α5(zeta) may exist in insect cells and undergo proteolysis at late stages in baculovirus infection. Except for the specific processing of α5(zeta), the 2D patterns shown in Fig. 5 did not reveal noticeable modification of CP subunits in the course of AcMNPV infection.

4. Discussion

In this report, we described for the first time the proteomic analysis of 26S proteasomes purified from insect cells. Due to the absence of annotated genes for most proteins of *S. frugiperda*, identification of proteasome subunits in Sf9 cells was based on a search of homologues in the NCBIall, NCBInr and Invertebrates_EST EST databases. Homologues of a total of 34 proteins that composed eukaryotic 26S proteasomes were identified in samples from Sf9 cells. General subunit composition and structure of 26S proteasomes from *Spodoptera* cells followed the pattern described for mammalian and yeast proteasomes with probably few exceptions. Homologues of RPN3/PSMD3 and small acidic subunit Sem1/DSS1 that links RPN3 to RPN7 [38] were not found in the purified samples. Meanwhile, the RPN2 (Sub.1), RPN7 (Sub. 6N), RPN8 (Sub. 7N) and RPN12 (Sub. 8N) subunits that interact with RPN3 in the lid complex of

yeast proteasomes [8] were recognized. Among these subunits, RPN12 is thought to be added last during lid assembly [10]. It remains unclear, whether the absence of RPN3 and Sem1 reflects peculiarities of insect proteasomes or limitation of our experimental procedures. Factors involved in binding and processing of ubiquitinated proteins, RPN13, UCH-14/UBP6, UCH-L5/UCH37, and TRX, were present in lower molar amounts than other subunits of RP and CP particles in purified 26S proteasome samples (Fig. 2). It is possible that only a portion of RP particles in Sf9 cells was fully equipped with accessory subunits required for hydrolysis of ubiquitinated proteins as was suggested earlier for RPs lacking RPN13 [39]. Comparison of the α3 band between the 2D maps of the purified samples (Fig. 4B) and crude extracts (Fig. 5) shows that α3 might be modified during proteasome purification or that the antibody differentially recognizes the modified species and unmodified protein. Although we cannot exclude that the purification procedure might modify some proteasome subunits, it preserved the structural integrity and proteolytic activity of proteasomes (Fig. 1B, C) and provided functional complexes for analysis.

The subunit patterns in 2D gels for 26S proteasomes purified from control and AcMNPV-infected cells at 48 hpi did not reveal major changes due to virus infection except subtle changes in minor forms of some proteasome subunits (β3a, β1a, α1a, 8Na, and β7a). This result was in agreement with previous observation of unchanged distribution of Sf9 proteasomes in a native polyacrylamide gel for AcMNPV-infected cells up to 96 hpi [22]. Host cell proteasome activity is essential for progression of baculovirus infection cycle [21–23]. It is possible that baculoviral control over the ubiquitin proteasome system in infected cells was mostly directed to the ubiquitination pathway and did not include direct modification of proteasomes. Baculovirus genomes encode genes for ubiquitin ligases and for homologue of ubiquitin [19,20,40]. Preservation of these genes in their genomes suggests that their function may be important for the baculovirus infection cycle and the general success of baculoviruses in evolution.

5. Conclusions

The 26S proteasome was purified for the first time from cells of an insect species, fall armyworm *S. frugiperda*. It showed a typical structure of the 26S proteasome that was most completely studied in mammals and yeast. Most subunits of the 20S core particle (CP) and the 19S regulatory particle (RP), except RPN3 and Sem1, were identified by the search of homologues in bioinformatics databases. Infection of *S. frugiperda* Sf9 cells with the baculovirus AcMNPV had no apparent effect on the composition of the 26S proteasome but some subtle changes in subunits were visible for β3a, β1a, α1a, 8Na, and β7a that remain to be investigated. The results confirmed the structural integrity of 26S proteasome in insect cells during baculovirus infection. However, a portion of the α5(zeta) cellular pool presumably not associated with proteasomes was degraded at a late stage in infection.

Conflict of interest

The authors declare no conflict of interest.

Acknowledgments

We thank George Rohrmann for critical reading and comments on the manuscript and M.B. Evgen'ev for his interest in this project. Single particle electron microscopy studies were performed at User Facility Center and Biology Faculty EM Lab of Moscow State University. MALDI MS analysis was available due to PNG 5.13 MSU program. The research was supported by grants from the Russian Foundation for Basic Research to S.N.B. (14-04-00792) and to V.S.M (15-04-01990) and by a grant from the Russian Academy of Sciences (Cell and Molecular Biology Program) to M.B.E.

References

[1] D. Finley, H.D. Ulrich, T. Sommer, P. Kaiser, The ubiquitin–proteasome system of *Saccharomyces cerevisiae*, Genetics 192 (2012) 319–360.
[2] P.C. da Fonseca, J. He, E.P. Morris, Molecular model of the human 26S proteasome, Mol. Cell 46 (2012) 54–66.
[3] D. Finley, Recognition and processing of ubiquitin–protein conjugates by the proteasome, Annu. Rev. Biochem. 78 (2009) 477–513.
[4] K. Lasker, F. Forster, S. Bohn, T. Walzthoeni, E. Villa, P. Unverdorben, F. Beck, R. Aebersold, A. Sali, W. Baumeister, Molecular architecture of the 26S proteasome holocomplex determined by an integrative approach, Proc. Natl. Acad. Sci. U. S. A. 109 (2012) 1380–1387.
[5] R.J. Tomko Jr., M. Hochstrasser, Molecular architecture and assembly of the eukaryotic proteasome, Annu. Rev. Biochem. 82 (2013) 415–445.
[6] R. Sanchez-Lanzas, J.G. Castano, Proteins directly interacting with mammalian 20S proteasomal subunits and ubiquitin-independent proteasomal degradation, Biomolecules 4 (2014) 1140–1154.
[7] G. Ben-Nissan, M. Sharon, Regulating the 20S proteasome ubiquitin-independent degradation pathway, Biomolecules 4 (2014) 862–884.
[8] G.C. Lander, E. Estrin, M.E. Matyskiela, C. Bashore, E. Nogales, A. Martin, Complete subunit architecture of the proteasome regulatory particle, Nature 482 (2012) 186–191.
[9] F. Forster, J.M. Schuller, P. Unverdorben, A. Aufderheide, Emerging mechanistic insights into AAA complexes regulating proteasomal degradation, Biomolecules 4 (2014) 774–794.
[10] R.J. Tomko Jr., D.W. Taylor, Z.A. Chen, H.W. Wang, J. Rappsilber, M. Hochstrasser, A single alpha helix drives extensive remodeling of the proteasome lid and completion of regulatory particle assembly, Cell 163 (2015) 432–444.
[11] D. de Verteuil, T.L. Muratore-Schroeder, D.P. Granados, M.H. Fortier, M.P. Hardy, A. Bramoulle, E. Caron, K. Vincent, S. Mader, S. Lemieux, P. Thibault, C. Perreault, Deletion of immunoproteasome subunits imprints on the transcriptome and has a broad impact on peptides presented by major histocompatibility complex I molecules, Mol. Cell. Proteomics 9 (2010) 2034–2047.
[12] F. Geng, S. Wenzel, W.P. Tansey, Ubiquitin and proteasomes in transcription, Annu. Rev. Biochem. 81 (2012) 177–201.
[13] G. Durairaj, P. Kaiser, The 26S proteasome and initiation of gene transcription, Biomolecules 4 (2014) 827–847.
[14] L.L. Winkler, R.F. Kalejta, The 19S proteasome activator promotes human cytomegalovirus immediate early gene expression through proteolytic and nonproteolytic mechanisms, J. Virol. 88 (2014) 11782–11790.
[15] M.K. Isaacson, H.L. Ploegh, Ubiquitination, ubiquitin-like modifiers, and deubiquitination in viral infection, Cell Host Microbe 5 (2009) 559–570.
[16] J.K. Gustin, A.V. Moses, K. Fruh, J.L. Douglas, Viral takeover of the host ubiquitin system, Front. Microbiol. 2 (2011) 161.
[17] H. Luo, Interplay between the virus and the ubiquitin–proteasome system: molecular mechanism of viral pathogenesis, Curr. Opin. Virol. 17 (2015) 1–10.
[18] G.F. Rohrmann, Baculovirus Molecular Biology, third ed., 2013 [Internet] (http://www.ncbi.nlm.nih.gov/pubmed/24479205).
[19] N. Imai, N. Matsuda, K. Tanaka, A. Nakano, S. Matsumoto, W. Kang, Ubiquitin ligase activities of *Bombyx mori* nucleopolyhedrovirus RING finger proteins, J. Virol. 77 (2003) 923–930.
[20] S. Katsuma, S. Kawaoka, K. Mita, T. Shimada, Genome-wide survey for baculoviral host homologs using the Bombyx genome sequence, Insect Biochem. Mol. Biol. 38 (2008) 1080–1086.
[21] S. Katsuma, A. Tsuchida, N. Matsuda-Imai, W. Kang, T. Shimada, Role of the ubiquitin–proteasome system in *Bombyx mori* nucleopolyhedrovirus infection, J. Gen. Virol. 92 (2011) 699–705.
[22] Y.V. Lyupina, S.B. Abaturova, P.A. Erokhov, O.V. Orlova, S.N. Beljelarskaya, V.S. Mikhailov, Proteotoxic stress induced by *Autographa californica* nucleopolyhedrovirus infection of *Spodoptera frugiperda* Sf9 cells, Virology 436 (2013) 49–58.
[23] J. Xue, N. Qiao, W. Zhang, R.L. Cheng, X.Q. Zhang, Y.Y. Bao, Y.P. Xu, L.Z. Gu, J.D. Han, C.X. Zhang, Dynamic interactions between *Bombyx mori* nucleopolyhedrovirus and its host cells revealed by transcriptome analysis, J. Virol. 86 (2012) 7345–7359.
[24] H.C. Besche, W. Haas, S.P. Gygi, A.L. Goldberg, Isolation of mammalian 26S proteasomes and p97/VCP complexes using the ubiquitin-like domain from HHR23B reveals novel proteasome-associated proteins, Biochemistry 48 (2009) 2538–2549.
[25] S.J. Ludtke, P.R. Baldwin, W. Chiu, EMAN: semiautomated software for high-resolution single-particle reconstructions, J. Struct. Biol. 128 (1999) 82–97.
[26] M. van Heel, G. Harauz, E.V. Orlova, R. Schmidt, M. Schatz, A new generation of the IMAGIC image processing system, J. Struct. Biol. 116 (1996) 17–24.
[27] P.Z. O'Farrell, H.M. Goodman, P.H. O'Farrell, High resolution two-dimensional electrophoresis of basic as well as acidic proteins, Cell 12 (1977) 1133–1141.
[28] Y.V. Lyupina, O.G. Zatsepina, A.V. Timokhova, O.V. Orlova, M.V. Kostyuchenko, S.N. Beljelarskaya, M.B. Evgen'ev, V.S. Mikhailov, New insights into the induction of the heat shock proteins in baculovirus infected insect cells, Virology 421 (2011) 34–41.
[29] U.K. Laemmli, Cleavage of structural proteins during the assembly of the head of bacteriophage T4, Nature (London) 227 (1970) 680–685.
[30] C. Enenkel, Using native gel electrophoresis and phosphofluoroimaging to analyze GFP-tagged proteasomes, Methods Mol. Biol. 832 (2012) 339–348.
[31] T. Shibatani, E.J. Carlson, F. Larabee, A.L. McCormack, K. Fruh, W.R. Skach, Global organization and function of mammalian cytosolic proteasome pools: implications for PA28 and 19S regulatory complexes, Mol. Biol. Cell 17 (2006) 4962–4971.
[32] L.W. Lee, C.R. Moomaw, K. Orth, M.J. McGuire, G.N. DeMartino, C.A. Slaughter, Relationships among the subunits of the high molecular weight proteinase, macropain (proteasome), Biochim. Biophys. Acta 1037 (1990) 178–185.

[33] K.S. Lilley, M.D. Davison, A.J. Rivett, N-terminal sequence similarities between components of the multicatalytic proteinase complex, FEBS Lett. 262 (1990) 327–329.
[34] L. Jiao, S. Ouyang, N. Shaw, G. Song, Y. Feng, F. Niu, W. Qiu, H. Zhu, L.W. Hung, X. Zuo, V. Eleonora Shtykova, P. Zhu, Y.H. Dong, R. Xu, Z.J. Liu, Mechanism of the Rpn13-induced activation of Uch37, Protein Cell 5 (2014) 616–630.
[35] R.T. VanderLinden, C.W. Hemmis, B. Schmitt, A. Ndoja, F.G. Whitby, H. Robinson, R.E. Cohen, T. Yao, C.P. Hill, Structural basis for the activation and inhibition of the UCH37 deubiquitylase, Mol. Cell 57 (2015) 901–911.
[36] A. Aufderheide, F. Beck, F. Stengel, M. Hartwig, A. Schweitzer, G. Pfeifer, A.L. Goldberg, E. Sakata, W. Baumeister, F. Forster, Structural characterization of the interaction of Ubp6 with the 26S proteasome, Proc. Natl. Acad. Sci. U. S. A. 112 (2015) 8626–8631.
[37] L. Jørgensen, K.B. Hendil, Proteasome subunit zeta, a putative ribonuclease, is also found as a free monomer, Mol. Biol. Rep. 26 (1999) 119–123.
[38] S. Bohn, E. Sakata, F. Beck, G.R. Pathare, J. Schnitger, I. Nagy, W. Baumeister, F. Forster, Localization of the regulatory particle subunit Sem1 in the 26S proteasome, Biochem. Biophys. Res. Commun. 435 (2013) 250–254.
[39] D. Berko, O. Herkon, I. Braunstein, E. Isakov, Y. David, T. Ziv, A. Navon, A. Stanhill, Inherent asymmetry in the 26S proteasome is defined by the ubiquitin receptor RPN13, J. Biol. Chem. 289 (2014) 5609–5618.
[40] L.A. Guarino, Identification of a viral gene encoding a ubiquitin-like protein, Proc. Natl. Acad. Sci. U. S. A. 87 (1990) 409–413.